Hindawi
International Journal of Optics
Volume 2021, Article ID 8481146, 9 pages
https://doi.org/10.1155/2021/8481146

Research Article

Experimental Research on Automatic Alignment and Control Algorithm of Spatial Light-Fiber Coupling

Xizheng Ke[1,2,3] and Benkang Yin[1]

[1]*Xi'an University of Technology, School of Automation and Information Engineering, Xi'an, Shaanxi, China*
[2]*Shaanxi Civil-Military Integration Key Laboratory of Intelligence Collaborative Networks, Xi'an, Shaanxi, China*
[3]*Shaanxi University of Technology, School of Physics and Telecommunications Engineering, Hanzhong, Shaanxi, China*

Correspondence should be addressed to Benkang Yin; 2180320103@stu.xaut.edu.cn

Received 7 April 2021; Accepted 24 May 2021; Published 1 June 2021

Academic Editor: Sulaiman W. Harun

This study aims to solve the difficulties in the coupling between space light and single-mode fiber (SMF) in free-space optical communication. A fiber coupler based on two-dimensional (2D) piezoelectric ceramics was developed, which uses the stochastic parallel gradient descent (SPGD) algorithm to realize the automatic coupling of space light-SMF. In addition, a spatial light-SMF alignment experimentation platform was built indoors to verify the effectiveness and practicality of the 2D piezoelectric ceramic fiber coupler. The results show that the use of the SPGD algorithm can realize the automatic alignment of fiber position coupling, and the SMF coupling efficiency reaches 52.58% when the system is closed loop. 2D piezoelectric ceramic fiber couplers have unique advantages of low cost, simplified structure, and easy array expansion and can effectively solve the difficulty in the alignment of spatial light-SMF coupling. This study will serve as a significant reference for the research on spatial fiber-coupled array technology.

1. Introduction

Free-space optical communication (FSOC) has broad application prospects in military and civil applications due to its high transmission speed, large information transmission capacity, strong confidentiality, and antielectromagnetic interference and has also become a research hotspot. Space optical coupling technology is a key technology in FSOC technology. The efficient and stable coupling of space light into optical fiber is the key to ensuring communication efficiency and decoding the success rate of the receiving system [1]. The spatial light-fiber coupling is affected by factors, such as atmospheric turbulence, platform jitter, and alignment deviation between the fiber end face and focus spot [2, 3]. Therefore, improving the coupling efficiency of space light to single-mode fiber (SMF) by suppressing atmospheric turbulence, compensating for random jitter, and correcting alignment deviation is a key technology in the field of high-speed laser communication.

In 2012, Takenaka et al. [4] designed a fast mirror that can work at high frequencies under the atmospheric turbulence condition, verified the tracking characteristics of the spot position in the spatial optical coupling, and improved the efficiency of optical fiber coupling by compensating the jitter error caused by atmospheric turbulence. In 2015, Chen et al. [5] used the Shack–Hartmann wavefront sensor to obtain the wavefront information of the spatial beam and used adaptive optics technology based on deformable mirrors and fast mirrors to correct the wavefront distortion caused by atmospheric turbulence. To improve the fiber coupling efficiency, the coupling efficiency after using a system a closed-loop system reached 46.1%. In [6], Chen et al. used a stepper motor to drive single-mode quartz fiber and single-mode plastic fiber using a charge-coupled device and optical power meter to feed back image and power data and realized the precise coupling of two fibers through the control and processing part of the upper computer to drive the motor movement. In 2016, Gao et al. [7] proposed the

use of a fast reflector as an actuator for beam direction change and a laser nutation method to achieve the coupling and alignment of the spatial light focusing spot and SMF. The experimental results show that the system response rate using this method was 40 Hz. In 2018, Tottinger et al. [8] proposed an optical fiber position sensor method. The sensor consists of a microlens array printed on an optical fiber bundle. The optical fiber bundle is composed of a central SMF and six surrounding multimode fibers. The optical energy in the surrounding multimode fiber adjusts the fiber position, and the simulation results show that the coupling efficiency can reach up to 69%. However, this method cannot be easily implemented, and its practical application is difficult. In 2019, Zhu et al. [9] of Changchun Institute of Optics, Fine Mechanics and Physics, analyzed the influence of the change in laser nutation parameters on the coupling efficiency when a fast steering mirror was used as a coupling device. However, the bandwidth of the system is low due to the influence of the natural response frequency of the fast steering mirror. In 2020, Jin et al. [10] proposed a nutation coupling scheme based on peak power feedback and fast mirror. The nutation algorithm was used to control the fast steering mirror to realize fiber coupling. The results show that the maximum coupling range is 1 mrad under system tracking, and the coupling efficiency can reach 50%.

With the application of fiber-coupled array technology, researchers have found that the existing spatial light-fiber coupling scheme has disadvantages, such as poor reliability and inconvenient array expansion [11]. Moreover, the single-mode fiber (SMF) core diameter is very small (8–10 μm), and it is difficult to realize the coupling and alignment artificially [12]. Accordingly, the present study innovatively combined two-dimensional (2D) piezoelectric ceramics with intelligent algorithms and automatically determined the optimal coupling alignment position through algorithm optimization. Commonly used intelligent optimization algorithms were as follows: improved quantum-inspired cooperative coevolution algorithms with multistrategy (MSQCCEA), improved differential evolution algorithm with neighborhood mutation operators and opposition-based learning (NBOLDE) algorithm, deep Q network (DQN) algorithm, improved quantum evolutionary algorithm based on the niche coevolution strategy and enhanced particle swarm optimization (IPOQEA), improved quantum-inspired differential evolution with multistrategies (MSIQDE) algorithm, and stochastic parallel gradient descent (SPGD) algorithm [13–17]. The MSQCCEA, NBOLDE, DQN, IPOQEA, and MSIQDE algorithms are suitable for solving complex optimization problems and have many parameters. In particular, the SPGD algorithm can directly optimize the system index, and a few algorithm parameters can reduce the complexity of the control system. Accordingly, this study used the SPGD algorithm combined with piezoelectric ceramics to realize the automatic alignment of spatial optical coupling.

2. SMF Coupling Theory Model

The principle of spatial light-SMF coupling is illustrated in Figure 1. For the principle diagram, the plane light wave is focused by the receiving optical system to form a focused spot on the back focal plane. Spatial light-SMF coupling involves placing an SMF at the focused spot to make the fiber core coincide with the spot. The calculation formula for the coupling efficiency is [18]

$$\eta = \frac{\left|\iint_A E_A^*(r)F_A(r)r\mathrm{d}r\mathrm{d}\theta\right|^2}{\iint_A \left|E_A(r)\right|^2 r\mathrm{d}r\mathrm{d}\theta \iint_A \left|F_A(r)\right|^2 r\mathrm{d}r\mathrm{d}\theta}, \tag{1}$$

where $E_A(r)$ is the light field distribution on the plane of the receiving lens and $F_A(r)$ is the mode field distribution of the SMF on the plane of the receiving lens. Because an SMF can only transmit the fundamental mode [19], the electromagnetic field distribution of the fundamental mode on the fiber end face is a zero-order Bessel function. A Gaussian distribution can be used to approximate the fundamental-mode field distribution [20]:

$$F_{\mathrm{GA}}(r) = \sqrt{\frac{2}{\pi}}\,\frac{1}{\omega_m}\exp\left[-\left(\frac{r}{\omega_m}\right)^2\right]. \tag{2}$$

In the FSO communication system, after a laser with a Gaussian distribution of light intensity is transmitted over a long distance, the light wave can be approximated as a plane wave. Without considering the influence of the coupling lens aberration using the Fresnel diffraction formula, the light field of the incident beam at the focal plane of the coupling lens can be expressed as [21]

$$E_{\mathrm{GA}}(r) = \frac{1}{i\lambda f}\exp(\mathrm{ikf})\exp\left(\frac{\mathrm{ikr}^2}{2f}\right)\pi\left(\frac{D_A}{2}\right)^2\left[\frac{2J_1(\pi D_A r/\lambda f)}{\pi D_A r/\lambda f}\right], \tag{3}$$

where f is the focal length of the coupling lens, D_A is the diameter of the coupling lens, J_1 (.) is the first-order Bessel function of the first kind, and $k = 2\pi/\lambda$ is the wave vector. A radical deviation exists between the fiber end face and the focused spot. At this time, the light field distribution of the parallel beam at the focal plane can be expressed as

$$F_{\mathrm{GA}}(r, \Delta r) = \sqrt{\frac{2}{\pi}}\,\frac{1}{\omega_m}\exp\left[-\left(\frac{r+\Delta r}{\omega_m}\right)^2\right], \tag{4}$$

where $\Delta r = \sqrt{\Delta x^2 + \Delta y^2}$ is the offset of the fiber end face. Combining equations (1), (3), and (4), the SMF coupling efficiency expression when the fiber position is laterally offset Δr is

$$\eta_{\Delta r} = \frac{\left|\int_0^{\infty} 1/-i\exp(-\mathrm{ikr})\exp\left(-\mathrm{ikr}^2/2f\right)\exp\left[-\left(r+\Delta r/w_0\right)\right]J_1\left(\pi D_A r/\lambda f\right)\mathrm{d}r\right|^2}{\int_0^{\infty}\left[J_1\left(\pi D_A r/\lambda f\right)\right]^2/r\mathrm{d}r\int_0^{\infty}\exp\left[-2\left(r+\Delta r/w_0\right)^2\right]r\mathrm{d}r}. \quad (5)$$

The laser wavelength was 1550 nm, the focus lens diameter was 5 mm, the focal length was 20 mm, and the SMF mode field radius was 5.25 μm. The simulation curve of the coupling efficiency of the SMF with the fiber radial offset is shown in Figure 2.

If the position of the fiber end face in the focused spot can be quickly and accurately controlled, then the effect of static alignment deviation on the coupling efficiency of the fiber and the effect of platform vibration on the coupling efficiency can be compensated, thereby achieving high efficiency and stable spatial light-SMF coupling.

3. System Structure and Control Algorithm

3.1. 2D Piezoelectric Ceramic and SMF Connector Structure. The working principle of 2D piezoelectric ceramics is shown in Figure 3(a). By utilizing the piezoelectric effect of piezoelectric ceramics and applying a corresponding control voltage to the displacement control end of the piezoelectric ceramics, microdisplacement can be achieved within the range shown in the figure. Figure 3(b) shows our SMF-coupled device based on a 2D piezoelectric ceramic design. The piezoelectric ceramic displacement end and the SMF end face were fixed to each other through a designed connector, and the position of the fiber end face was adjusted through the displacement of the piezoelectric ceramic.

3.2. Spatial Light-SMF Coupling Automatic Alignment System. The structure diagram of the SMF coupling automatic alignment system based on 2D piezoelectric ceramics is shown in Figure 4. The optical system is composed of a laser, a collimating lens, a coupling lens, and an SMF, and the closed-loop control system consists of 2D piezoelectric ceramics, an optical power meter, a controller, a digital-to-analog converter, and high-voltage amplifier modules. When the system is working, the optical power meter collects the optical power coupled to the SMF in real time as the performance evaluation index of the system, and the control processor generates a set of control signals according to the evaluation index. The control signal is amplified by a digital-to-analog converter and high-voltage amplifier modules to drive the 2D piezoelectric ceramics to produce microdisplacement. The SPGD algorithm maximizes the evaluation function, and the optical fiber end face achieves the optimal coupling alignment attitude.

3.3. Control System Hardware Structure and Algorithm. The hardware structure of the entire control system is shown in Figure 5. The piezoelectric ceramic drive part is composed of a constant-voltage power supply module and a high-voltage amplifier module. The constant-voltage power supply module provides the working voltage for the piezoelectric ceramics, and the high-voltage amplifier module linearly amplifies the control signal to control the displacement of the piezoelectric ceramics. The field-programmable gate array (FPGA) module realizes the reception of control commands and drives the output of the DA module. The optical power meter realizes real-time power collection and uploads it to the control system. The control system runs the algorithm. The FPGA part uses ALTERA Cyclone IV EP4CE15F23C8 as the core control board, and the digital-to-analog conversion part uses Analog Device's AD9767, which supports up to 125 MHz clock and 14-bit precision. When the system is working, the PC sends a set of initial voltage control signals to the FPGA module through the serial port, and the FPGA drives the DA module to output the corresponding voltage to control the 2D piezoelectric ceramics through a high-voltage amplification.

The SMF automatic coupling alignment system adopts the SPGD algorithm to perform the following steps:

(1) Initialization: randomly generate a set of initial control voltage signals $U_0 = [u_1, u_2, \ldots, u_N]$, where u_N correspond to the output voltage of the Nth channel of the DA module.

(2) Generating disturbance: generate a set of randomly disturbed voltage signals $\Delta u_i = [\sigma u_1, \sigma u_2, \ldots, \sigma u_N]$, where σu_N corresponds to the random disturbance voltage of the Nth channel, which satisfies Δu_i mutual independence and obeys the Bernoulli distribution.

(3) Load the voltage sequence $U_0 + \Delta u_i$ on the piezoelectric ceramic of the actuator, take the feedback coupled optical power as the system evaluation function and record it as $J_+^{(i)}$.

(4) Load the voltage sequence $U_0 - \Delta u_i$ on the piezoelectric ceramic of the actuator, take the feedback coupled optical power as the system evaluation function and record it as $J_-^{(i)}$.

(5) Calculate the variation of the evaluation function $\delta J^{(i)} = \delta J_+^{(i)} - \delta J_-^{(i)}$.

(6) Control voltage update: according to the voltage iteration formula $U_{i+1} = U_i - \mu\delta J^{(i)}\Delta u_i$, update the control voltage and calculate U_{i+1}. If the corresponding system performance evaluation function value J^i does not meet the system requirements, repeat steps 2–6 until the system's requirements for the evaluation function are met. μ is the iteration step parameter.

From the implementation process of the above SPGD algorithm, it can be seen that the gain coefficient μ and disturbance voltage Δu are important parameters of the algorithm. Simulate the effects of different gain coefficients and different disturbance voltages on the performance of the algorithm. When $\mu = 50$, the variation curve of the coupling efficiency with the number of iterations at different

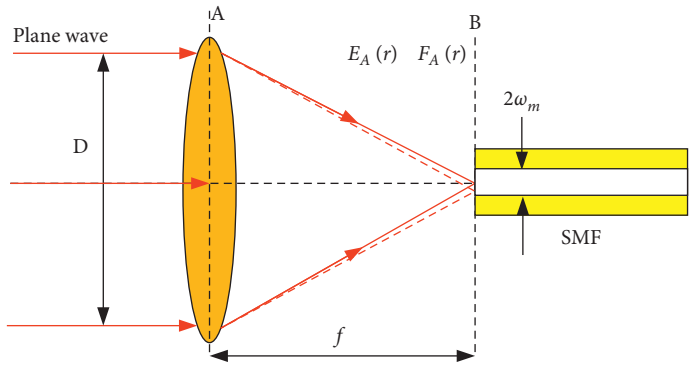

Figure 1: Schematic diagram of plane wave coupling to SMF.

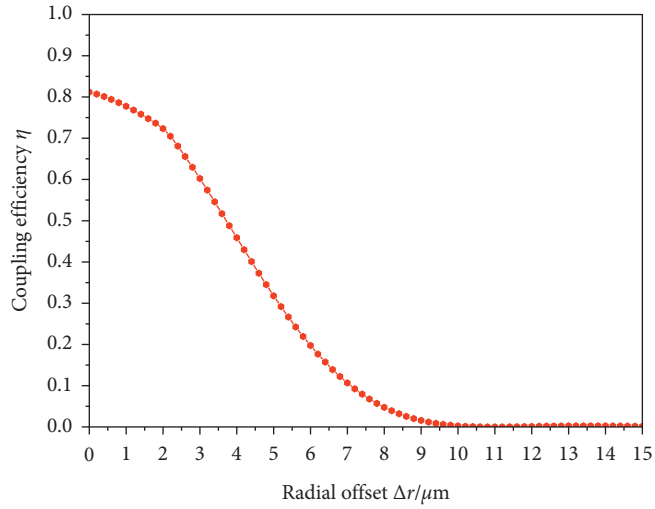

Figure 2: Relationship between the coupling efficiency and fiber offset.

disturbance voltages Δu is as shown in Figure 6(a). When $\Delta u = 0.02$, the conversion curve of the coupling efficiency with the number of iterations at different gain coefficients μ is as shown in Figure 6(b).

Figure 6(a) shows that when the disturbance voltage is small, the algorithm needs more iterations for convergence. When the iterative process tends to be stable, the number of iterations for algorithm convergence decreases with the increase of disturbance voltage. However, the stationarity of the iterative process is weakened. Figure 6(b) shows that when the gain coefficient is small, the number of iterations required for the algorithm convergence is large, but the coupling efficiency of the iterative process fluctuates less. With the increase in the gain coefficient, the number of iterations required for the algorithm convergence decreases. The fluctuation of coupling efficiency increases during the iteration process. Because the SPGD algorithm estimates the direction of the gradient through the disturbance voltage, in practical applications, when the disturbance voltage is large, although the algorithm can converge faster, it will cause the stability of the convergence to weaken. In general, a small disturbance voltage is selected to improve the stability of the algorithm, and the convergence speed of the algorithm is improved by selecting the appropriate gain coefficient. Therefore, $\mu = 50$ and $\Delta u = 0.02$ are chosen as the parameters of the algorithm in the experiment.

4. Experimental Research

To verify the effectiveness of the designed coupling device and its control algorithm, a spatial light-fiber coupling automatic alignment experiment system based on 2D piezoelectric ceramics was built, as shown in Figure 7.

The experimental devices used in the SMF coupling automatic alignment experiment are listed in Table 1.

In the experiment, the emission power of the narrow-linewidth laser was 10 mW, and the algorithm parameters were selected as the perturbation voltage $\Delta u = 0.02$ and iteration step size $\mu = 50$. The experimentally measured focal-plane optical power value was 2.36 mW, and the optical power sampling frequency was 50 Hz. The experimental process was as follows: the laser emitted by the laser was connected to the laser collimator through an SMF, and the collimated parallel light emitted from the collimator was focused through a coupled focusing lens. Because the wavelength of 1550 nm is nonvisible light, a photosensitive card was used to determine the position of the focusing spot. The piezoelectric ceramic coupler was installed on the three-

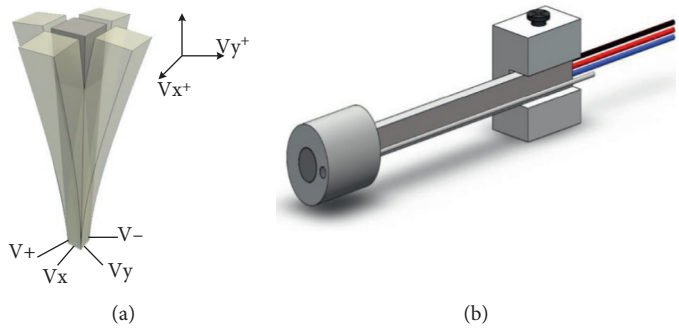

Figure 3: (a) Schematic diagram of a 2D piezoelectric ceramic displacement. (b) Piezoelectric ceramic and optical fiber connection structure.

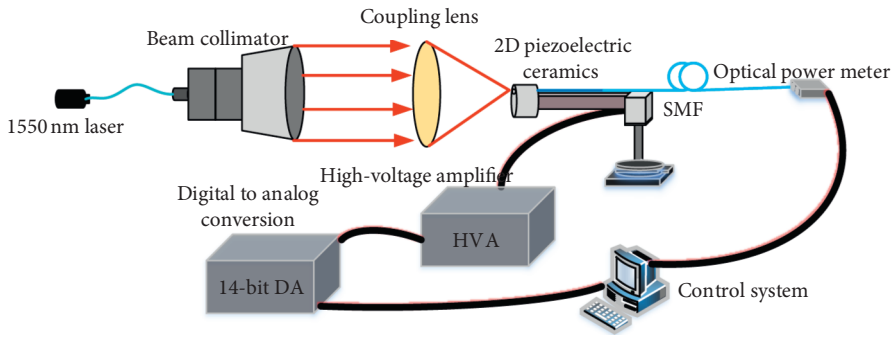

Figure 4: Schematic diagram of the spatial light-fiber coupling automatic alignment system.

dimensional manual microtranslation stage and completes the initial alignment of the optical fiber coupling by adjusting the stage. At this time, according to the power value in the optical power meter, the SPGD algorithm was run on a PC, and the control command was sent to the piezoelectric ceramic drive module through the serial port. The displacement of the piezoelectric ceramic was controlled to drive the displacement of the end face of the optical fiber. The evaluation index of the algorithm is the magnitude of the optical power coupled to the optical fiber.

Figure 8(a) is the curve of the coupling optical power versus time when the initial alignment coupling optical power is −3.2 dBm. When the system is open loop, the coupled optical power is small and greatly fluctuates. When the system is closed loop, the coupled optical power gradually increases. After 4.9 s, the system optical power tends to stabilize, and the coupling optical power fluctuates less at this time. Figure 8(b) is the curve of the coupling optical power versus time when the initial alignment coupling optical power is 0.4 dBm. When the system is open loop, the coupling optical power greatly fluctuates. When the algorithm system enters the closed-loop state, the coupling optical power gradually approaches the maximum. After 1.8 s, the coupling power tends to be stable, and the fluctuation of power is smaller than that of the open-loop state. By comparing the coupling efficiency with time in different initial states, it can be seen that when the initial coupling optical power is closer to the maximum, the convergence time of the algorithm is shorter, and the convergence speed is faster. Moreover, the coupling optical power and power stability of the system will be improved after the closed-loop state, which shows the effectiveness of the algorithm.

Figure 9 shows the transformation curve of the coupling efficiency with time when the initial coupled optical power is −3.2 dBm and 0.4 dBm. When the system is open loop, the maximum coupling efficiency is 21.73% and 47.54%. When the system is closed loop, the coupling efficiency gradually increases. When the closed-loop system is stable, the maximum coupling efficiency reaches 52.9%. After the closed-loop system becomes stable, the coupling efficiency is stable, and the fluctuation is significantly reduced, indicating that the algorithm can improve the coupling efficiency and stability of the coupling efficiency.

Table 2 shows the results of the open-loop and closed-loop states of the system when the initial coupling power is −3.2 dBm and 0.4 dBm, respectively. This study used the standard deviation of the coupled optical power to evaluate the stability of the closed-loop system. When the system is an open loop, the standard deviations of the coupled optical powers in the two different initial states are 0.089 dBm and 0.1183 dBm, respectively. When the system is a stable closed loop, the standard deviations of the coupled optical powers are 0.0249 dBm and 0.0247 dBm, respectively. The stability of the coupled power greatly improved after the closed-loop system was stabilized. When the system is open loop, the average coupling efficiencies in the two different initial states are 20.41% and 45.94%, respectively. When the system is a stable closed loop, the average coupling efficiency of the SMF

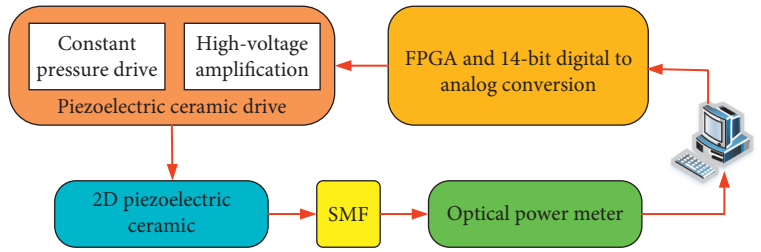

Figure 5: System hardware structure diagram.

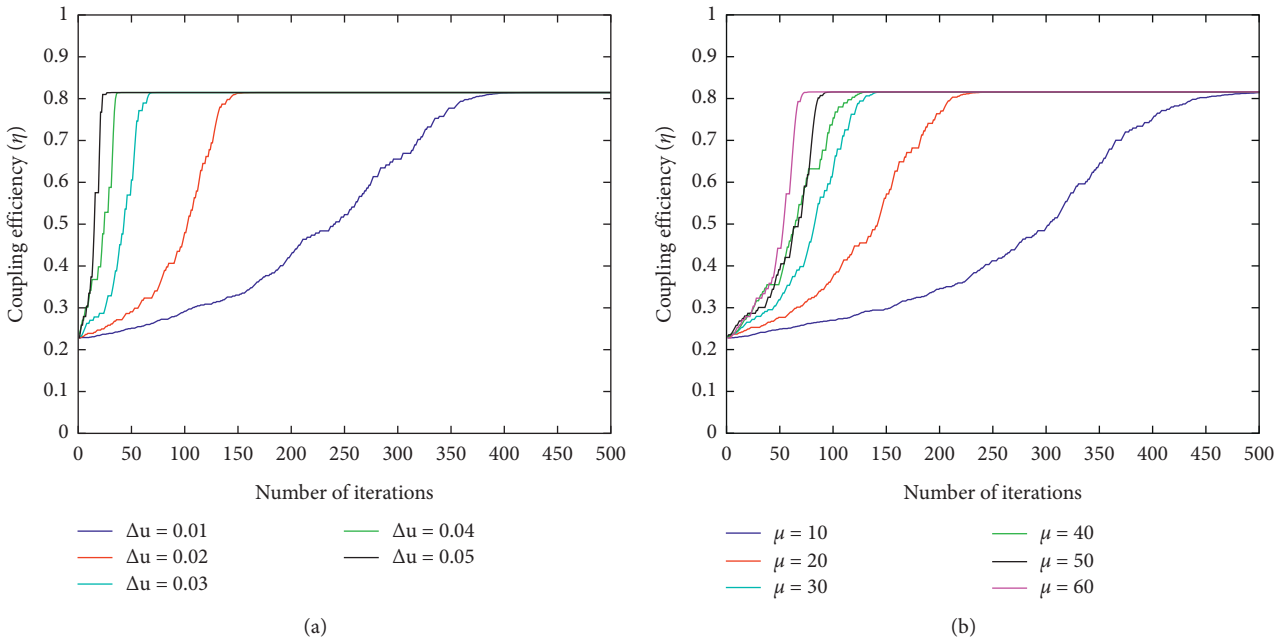

Figure 6: (a) Relationship between the coupling efficiency and the number of iterations under different disturbance voltages. (b) Relationship between the coupling efficiency and the number of iterations under different gain coefficients.

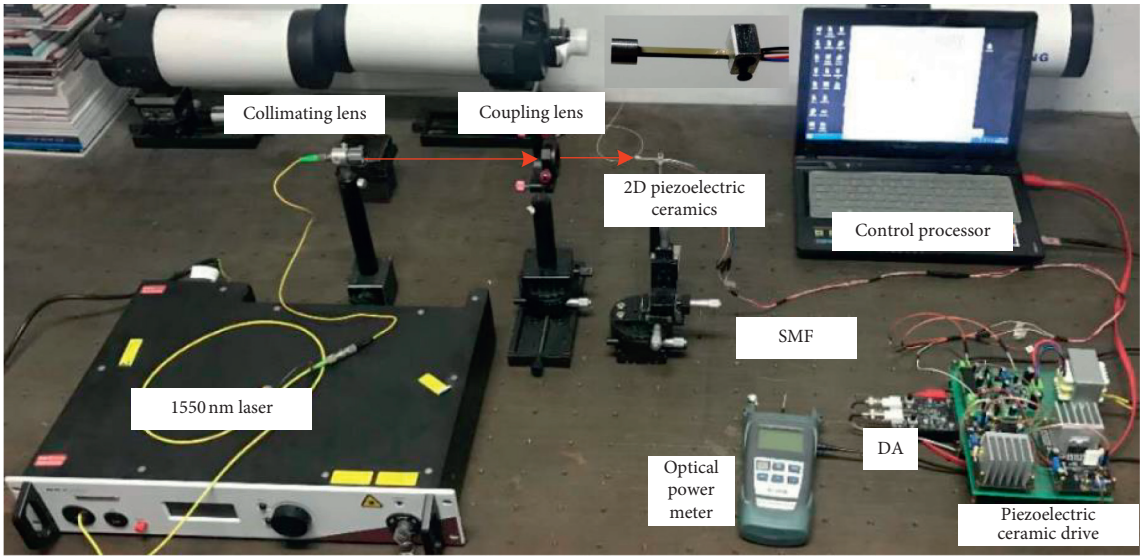

Figure 7: Physical image of the spatial light-fiber coupling automatic alignment system.

Table 1: Optical fiber coupling automatic alignment experimental device.

Device	Type	Main parameters
Laser	Koheras Adjustik E15	Wavelength: 1550 nm, linewidth: 0.1 kHz, output power: 0 ~ 200 mW
Coupling lens	GCL-0102	Wavelength: 1550 nm, focal length: 40 mm
2D piezoelectric ceramics	NAC2710	Working voltage: 60 V, stroke: 90 μm
Optical power meter	RY3200 B	Wavelength range: 850 ~ 1625 nm
Adjustment table	GCX—M0101FC	Provide X, Y, Z 10 μm accuracy
Fiber	Custom SMF	Wavelength range: 1550 ± 10 nm

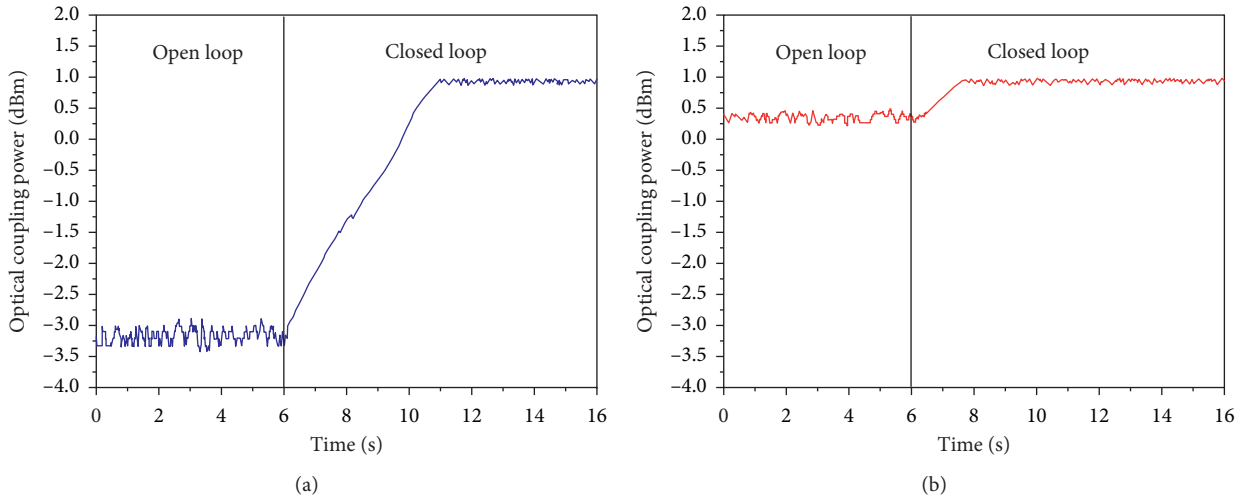

Figure 8: (a) Initial power of −3.2 dBm SMF-coupled optical power versus the time curve. (b) Initial power of 0.4 dBm SMF-coupled optical power versus the time curve.

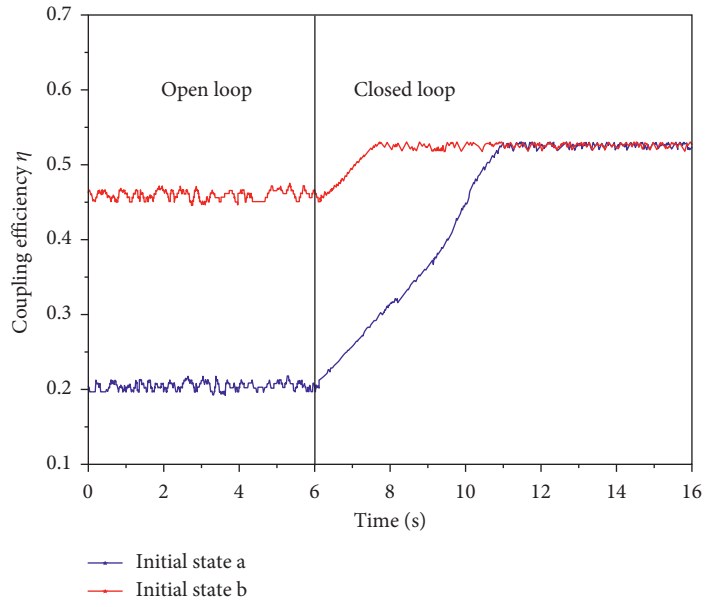

Figure 9: Open-loop and closed-loop coupling efficiency curves of the SMF coupling autoalignment system.

in both states is increased to approximately 52.5%. This finding shows that the coupling efficiency under different initial alignment conditions can be improved to a larger stable range by the algorithm. The actual measured coupling efficiency deviates from the theoretical value, which is mainly due to the Fresnel reflection of the end face of the optical fiber, absorption loss, and optical path error in the experiment.

Table 2: Comparison of the open- and closed-loop system results under different initial conditions.

Initial state	Open loop		Closed loop	
	Mean coupling efficiency	Power standard deviation (dBm)	Mean coupling efficiency	Power standard deviation (dBm)
a	0.2041	0.089	0.5256	0.0249
b	0.4594	0.1183	0.5258	0.0247

Compared with other methods used to realize spatial light coupling, the method adopted in this study directly adjusts the position of the optical fiber without introducing aberrations due to the change in the optical path. Compared with the motor and mechanical adjustment method, the designed piezoelectric ceramic coupling device has a faster response speed and can realize coupling automatic alignment in a short time. The use of piezoelectric ceramics can achieve a nanometre-level adjustment accuracy. At the same time, the method used in this study has a small structure and low cost and has potential applications in array expansion and integration. It can also be applied to array fiber coupling systems in the future.

5. Conclusions

In this study, a fiber-coupled actuator based on 2D piezoelectric ceramics was designed. Considering the high-precision microdisplacement characteristics of piezoelectric ceramics, the random parallel gradient descent algorithm was used to realize the spatial optical coupling automatic alignment experiment, and an SMF coupling alignment experiment with a wavelength of 1550 nm was performed. The experimental results show that the random parallel gradient descent algorithm has good practicability, can stabilize the optical power in a certain range under the alignment condition, and can be used to maintain the stability of optical power and improve the reliability of the communication system. This method is feasible and can locate optical fibers at the best coupling position. In the closed-loop system, the average coupling efficiency reached 52.58%. In addition, the coupling device used in this study has the advantages of low cost, compact structure, easy implementation, and convenient array expansion and can be applied in fiber-coupled array technology.

Data Availability

All data generated or analyzed during this study are included within this article.

Conflicts of Interest

The authors declare no conflicts of interest.

References

[1] B. Shuai, J. Wang, L. Zhang, and M. Yang, "Development history and trend of space optical communication," *Laser & Optoelectronics Progress*, vol. 52, no. 7, pp. 7–20, 2015.

[2] Z. Xiong, Y. Ai, S. Xin et al., "Coupling efficiency and compensation analysis of optical fiber for space optical communication," *Infrared and Laser Engineering*, vol. 42, no. 9, pp. 2510–2514, 2013.

[3] X. L. Li, *Research on the Influence of Space Light Offset Incidence on Optical Fiber Coupling Efficiency in Satellite Communication Terminal*, Master Thesis, Harbin Institute of Technology, Harbin, China, 2015.

[4] H. Takenaka, M. Toyoshima, and Y. Takayama, "Experimental verification of fiber-coupling efficiency for satellite-to-ground atmospheric laser downlinks," *Optics Express*, vol. 20, no. 14, pp. 15301–15308, 2012.

[5] M. Chen, C. Liu, and H. Xian, "Experimental demonstration of single-mode fiber coupling over relatively strong turbulence with adaptive optics," *Applied Optics*, vol. 54, no. 29, p. 8722, 2015.

[6] S. Chen, D. Yang, P. Fang, and Q. Liao, "Single-mode quartz fiber and plastic fiber automatic coupling system," *Semiconductor Optoelectronics*, vol. 27, no. 3, pp. 282–285, 2006.

[7] J. Gao, J. Sun, J. Li, R. Zhu, P. Hou, and W. Chen, "Coupling method of space light to single-mode fiber based on laser nutation," *Chinese Journal of Lasers*, vol. 43, no. 8, pp. 25–32, 2016.

[8] P. Hottinger, R. J. Harris, and P. I. Dietrich, "Micro-lens array as a tip-tilt sensor for single-mode fiber coupling," *Proceedings of SPIE*, vol. 10706, 2018.

[9] S. W. Zhu, L. Sheng, and Y. K. Liu, "Single-mode fiber laser nutation conversion algorithm based on energy feedback," *Chinese Journal of Lasers*, vol. 46, no. 2, pp. 165–170, 2019.

[10] Z. Jin, S. Tong, X. Yu et al., "Research on nutation coupling of single-mode fiber based on peak power feedback," *Chinese Journal of Lasers*, vol. 47, no. 11, pp. 209–216, 2020.

[11] F. Li, C. Geng, X. Li et al., "Co-aperture transceiving of two combined beams based on adaptive fiber coupling control," *Photonics Technology Letters*, vol. 27, 2015.

[12] S. Hong-Fei, C. Ying, Z. Xin, L. Peng-Fei, and Z. Ian-Hong, "Improvement of fiber coupling efficiency in atmospheric turbulence," *Optics and Precision Engineering*, vol. 22, no. 12, pp. 3205–3211, 2014.

[13] X. Cai, H. Zhao, S. Shang et al., "An improved quantum-inspired cooperative co-evolution algorithm with muli-strategy and its application," *Expert Systems with Applications*, vol. 171, Article ID 114629, 2021.

[14] W. Deng, S. Shang, X. Cai, H. Zhao, Y. Song, and J. Xu, "An improved differential evolution algorithm and its application in optimization problem," *Soft Computing*, vol. 25, no. 7, pp. 5277–5298, 2021.

[15] S. Guo, X. Zhang, Y. Du, Y. Zheng, and Z. Cao, "Path planning of coastal ships based on optimized DQN reward function," *Journal of Marine Science and Engineering*, vol. 9, no. 2, p. 210, 2021.

[16] W. Deng, J. Xu, H. Zhao, and Y. Song, "A novel gate resource allocation method using improved PSO-based QEA," *IEEE Transactions on Intelligent Transportation Systems*, pp. 1–9, 2020.

[17] W. Deng, J. Xu, X.-Z. Gao, and H. Zhao, "An enhanced MSIQDE algorithm with novel multiple strategies for global

optimization problems," *IEEE Transactions on Systems, Man, and Cybernetics: Systems*, pp. 1–10, 2020.

[18] L. Ma, *Study on the Influence of Atmospheric Turbulence on the Probability Distribution of Coupling Efficiency of Space Light to Single-Mode Fiber*, Master Thesis, Harbin Institute of Technology, Harbin, Heilongjiang, China, 2015.

[19] Y. B. Liao and M. Li, *Fiber Optics*, pp. 13–15, Tsinghua University Press, Beijing, China, 2013.

[20] S. C. Lei and X. Z. Ke, "Research on spatial light coupling efficiency of the lens array in atmospheric turbulence," *Chinese Journal of Lasers*, vol. 42, no. 6, pp. 179–186, 2015.

[21] K. Deng, B. Z. Wang, X. Wang et al., "Analysis of coupling efficiency factors of space light-single-mode fiber," *Journal of University of Electronic Science and Technology of China*, no. 5, pp. 889–891, 2007.